NANO LETTERS

2008
Vol. 8, No. 9
2806-2813

# Printing Highly Efficient Organic Solar Cells

**Claudia N. Hoth,*,†,‡ Pavel Schilinsky,*,† Stelios A. Choulis,*,†,§ and Christoph J. Brabec*,†**

*Konarka Technologies GmbH, Landgrabenstrasse 94, D-90443 Nürnberg, Germany, and Department of Energy and Semiconductor Research, University of Oldenburg, D-26129 Oldenburg, Germany*

*Received May 13, 2008; Revised Manuscript Received June 17, 2008*

## ABSTRACT

**The technological attraction in organic solar cells is their compatibility to printing processes. However, up to today, nearly no literature on "printed" organic solar cells have been published and the major body of the research work was done by spin coating or blading techniques. Transferring the spin-coating or doctor blading process currently used for the fabrication of bulk heterojunction solar cell to a printing process holds morphological challenges that have not been observed or reported up to today. We highlight these challenges and we show that inkjet printing of organic bulk heterojunction solar cells requires completely novel approaches and skill sets compared to the current state of the art. By adjusting the chemical properties of the poly(3-hexylthiophene) polymer donor and by using our recently developed inkjet solvent mixture, we have gained control over the nanomorphology of poly(3-hexylthiophene):fullerene blends during the printing process and report a new record power conversion efficiency of 3.5% for inkjet printed poly(3-hexylthiophene):fullerene based solar cells.**

During the last five years, increasing concern about global warming has led to an intense search for cost-effective alternative energy sources such as photovoltaics. In particular, organic photovoltaic devices[1–3] have the virtue of being lightweight and flexible and could open up many new applications for solar cells, ranging from self-powered electronic newspapers to self-sufficient buildings.[4] Because organic and molecular materials can be processed by solutions at low temperatures, this may allow for the printing of organic solar cells. The application of printing technology as a fabrication tool for organic photovoltaics indicates the potential of these novel materials for future light-activated power plastic sources. At present bulk heterojunction structures (BHJ) based on blends, polymer donor and a fullerene acceptor, have been among the materials systems with the highest reported efficiencies, but the performance depends critically on the properties of the materials and processing conditions affecting the blend morphology.[5–7] For over a decade the first BHJ devices were reported, all significant improvements in their power conversion efficiency occurred by control over their morphological properties. It has been observed that the morphology of the polymer:fullerene blends can be influenced by the choice of solvent,[8–10] annealing conditions,[11–14] drying rate,[15] chemical properties of the polymer donor[16–18] and incorporation of additives.[19] However, all the part of the published work so far has been done by spin coating or blading processes which are not ideal techniques for exploring the full potential for the production of organic solar cells. Among other printing technologies recently implemented for the fabrication of organic electronic devices, such as gravure[25] or screen printing,[26] the inkjet printing technique is very promising due to the compatibility with various substrates because the ink material is transferred from the writing head to the substrate without direct contact with the surface.[26] Defined areas can be precisely printed with high resolution very easily by drop on demand (DOD) and thus, a postpatterning of the coated layer can be eliminated. The DOD technology provides easy patterning of the functional layers which is necessary concerning the interconnection of solar cell modules, where adjacent cells are electrically connected to each other in series. Recently certified 5.21% power conversion efficiency (PCE) large area organic solar cell have been demonstrated from Konarka Technologies (Certified by National Renewable Energy Laboratory (NREL) from Nov 2006) and identification of suitable printing methods for production of organic photovoltaics is regarded as the next important milestone.

In this contribution we show that in the case of polymer:fullerene blends the morphology formation for the inkjet printing process is fundamentally different to the film forming after a blading or spin coating process and that inkjet printing

* Corresponding authors. E-mail: C.N.H. and P.S., cklepek@konarka.com; S.A.C., schoulis@konarka.com; C.J.B., cbrabec@konarka.com.
† Konarka Technologies GmbH.
‡ University of Oldenburg.
§ Present address: Department of Mechanical Engineering and Materials Science and Engineering, Cyprus University of Technology, 3603 Limassol, Cyprus.

10.1021/nl801365k CCC: $40.75 
**Published on Web 08/07/2008**

of organic bulk heterojunction solar cells requires completely novel approaches and skill sets compared to the current state of the art. We further show that in the case of printing and in particular inkjet printing, the common solvents,[8–10,20] drying conditions[11–15,20] and chemical properties for regioregular (RR) poly(3-hexylthiophene) (P3HT):methanofullerene (PCBM) [17,18,20] solar cells previously reported for optimized devices fabricated by spin coating or doctor blading techniques can not be used to provide adequate nanomorphology for the inkjet printing technology. Previous work on organic field effect transistors and fluorescence organic light emitting diodes using inkjet printers have not observed similar limitations, because such devices they usually do not require a two component active material system.

Besides the choice of the solvent and the processing conditions, the morphological properties of an inkjet printed P3HT:PCBM active layer demands proper design of the regioregularity (RR) of the polymer donor. The RR needs to be chosen to extend the gelation time of the RR-P3HT:PCBM blend, and the choice of the solvent formulation should allow a higher drying rate of the wet bulk with a coating at low deposition temperatures (we discuss these points in more details later in the text). By using a combination of 96% RR-P3HT and our recently developed oDCB/mesitylene solvent formulation,[21] we have achieved improved solar cell device performance with a power conversion efficiency (PCE) of 3.5%.

Critical parameters for the production of highly efficient organic solar cells by printing are the inkjet latency time (effect of gelation), the inkjet printing table temperature, the effect of drying related to both inkjet table temperature and solvents and the effect of the chemical properties of the polymer donor. To highlight the scientific and technological challenges for highly efficient inkjet printed organic solar cells, we discuss all the above parameters strongly affecting the morphology of inkjet printed organic BHJ solar cells with equivalent cells made by more conventional processing methods such as doctor blading.

We found that we can gain control of the inkjet latency time (see inkjet printing methods section) of the RR-P3HT:PCBM formulation by altering the regioregularity (RR) of P3HT. As an initial step we focus our studies on two blend solutions using PCBM as electron acceptor but differing in the regioregularity properties of the P3HT donor. Pristine P3HT and pristine PCBM solutions with solid concentrations of 2 wt % of RR-P3HT and 2 wt % PCBM and combined in the ratio of 1:1 by volume[10–17,20] were prepared using RR-98.5% P3HT and RR-93% P3HT and initially dissolved in tetralene and the molecular weight distribution ($M_w$) of the two P3HT donor materials was constant at 73000. Importantly we note that tetralene provides slow drying conditions, which result in the case of spin-coated RR-P3HT:PCBM with favorable morphology and enhances the PCE performance of RR-P3HT:PCBM.[14] We show later in the text that in contrast to spin-coating technique the inkjet printing requires rapid drying for efficient solar cells performance.

Figure 1a,b demonstrates the atomic force microscopy (AFM) images of the RR-98.5% (1a) and RR-93% (1b) P3HT:PCBM inkjet printed films using tetralene as a solvent. Due to the different regioregularities and therefore inkjet printing properties, a significant distinction in the grain size and surface roughness between the inkjet printed layers of RR-98.5%-P3HT:PCBM and RR-93%-P3HT:PCBM is visible. The AFM images of the inkjet printed RR-98.5%-P3HT:PCBM display significantly rough surface for the inkjet printed active region. The rms roughness is calculated to be 73 nm for the inkjet RR-98.5%-P3HT:PCBM tetralene formulation, but the rms roughness could be reduced to 26 nm using a RR-93%-P3HT:PCBM tetralene based inkjet solution. Due to the high surface roughness of the RR-98.5%-P3HT:PCBM film the average film thickness is 300 nm $\pm$72 nm. The nonuniform film thickness and the larger grain size of the RR-98.5%-P3HT:PCBM compared to RR-93%-P3HT:PCBM inkjet printed layer from tetralene indicates morphological limitations for the RR-98.5%-P3HT:PCBM, which can be attributed to gelation of the RR-98.5%-P3HT:PCBM solution within the inkjet printing dwell time (see inkjet printed solar cell fabrication and characterization section).

The latency time for which printing can be stopped without modifications of the solution was in the range of 5 min for the RR-98.5%-P3HT:PCBM, too short for the inkjet printing process, and the RR-93%-P3HT:PCBM exhibited a latency time up to 1 h. The chemical modification (gelation) for RR-98.5%-P3HT:PCBM was confirmed during the inkjet printing process because after a short printing interval and as soon as the temperature of the solution in the ink reservoir was decreased the nozzles were clogged. The dwell time for a continuous printing of the RR-98.5%-P3HT:PCBM was only 30 min, whereas the printing of the RR-93%-P3HT:PCBM tetralene formulation could proceed for a couple of hours. The morphological limitations of the inkjet printed RR-98.5%-P3HT:PCBM from tetralene due to short inkjet latency time (fast gelation), creating demixing of the materials within the blend were also confirmed in the device performance. Solar cell devices based on ITO/doctor bladed PEDOT:PSS/inkjet printed with inkjet table temperature of 60 °C and RR-98.5%-P3HT:PCBM from tetralene/Ca:Ag under calibrated AM 1.5 conditions show a PCE of only 0.73% due to low values of Jsc and FF (see Figure 1 in the Supporting Information).

Besides the choice of solvents, the drying process of the blend solution and thus, the morphological properties is influenced by the inkjet and doctor blading table temperature. For the RR-98.5%-P3HT:PCBM blend the temperature was set to 60 °C the same temperature used for our optimized devices prepared by doctor blading. For the RR-93%-P3HT:PCBM blend table temperatures above 40 °C resulted in the accumulation of the solution in the center of the substrate, creating a very rough and thick layer in the micrometer scale in the middle and a pile-up of very low concentrated solution resulting in an ultrathin layer at the edges.[21] Due to this limitation on the film uniformity, the inkjet table was heated to 40 °C for the RR-93%-P3HT:PCBM in tetralene, whereas

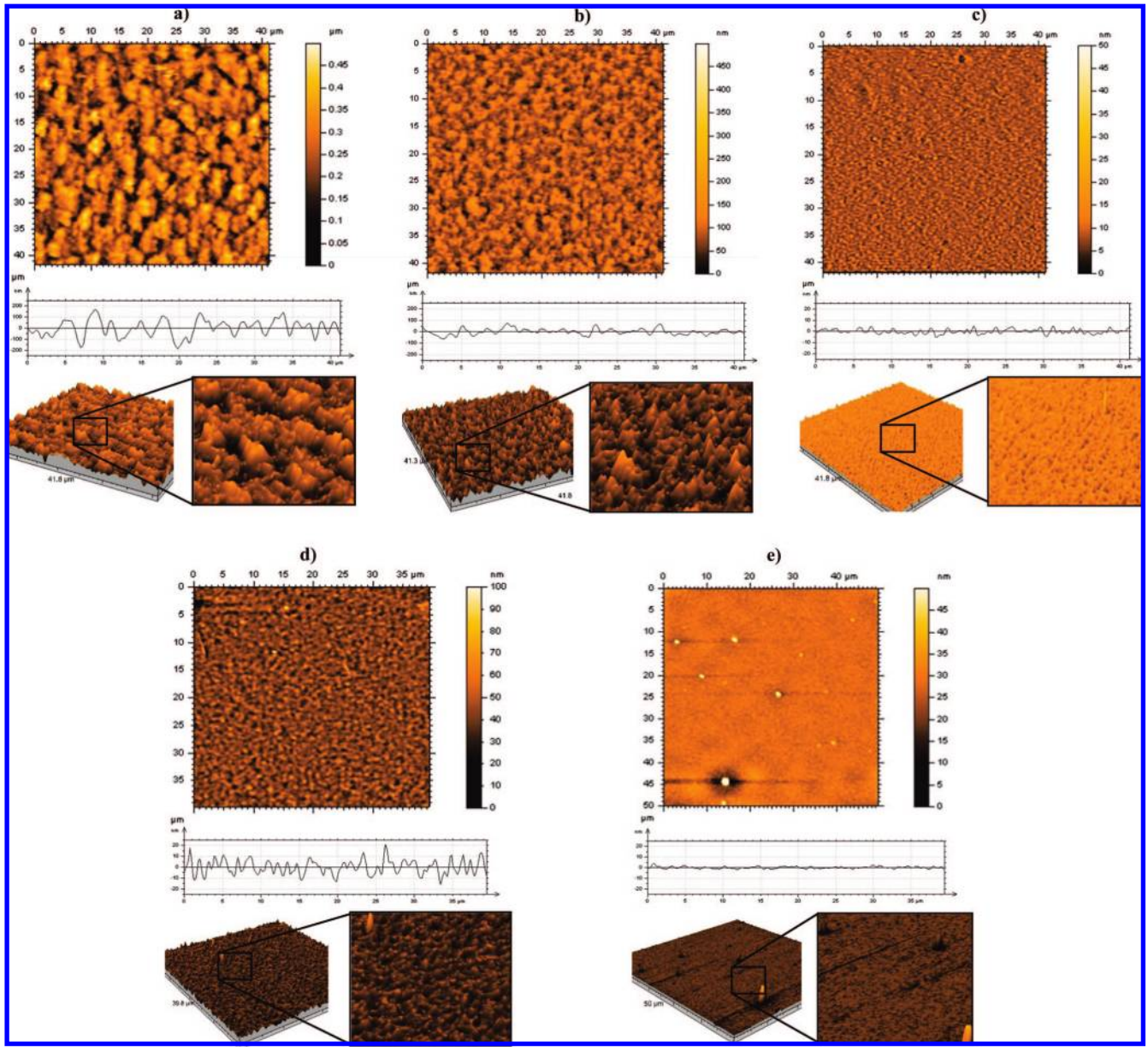


**Figure 1.** Atomic force microscopy images of a 40 by 40 $\mu$m scanned area representing the surface topographies, roughness profiles and the spatial geometry of the devices under study. (a) Inkjet printed RR-98.5%-P3HT:PCBM device based on tetralene. (b) Inkjet printed RR-93%-P3HT:PCBM based on tetralene. For both images (a) and (b) the height amplification is adjusted to 500 nm (c) doctor bladed RR-93%-P3HT:PCBM based on tetralene. Due to the improved uniformity, the resolution is chosen to a 50 nm height scale. (d) Inkjet printed RR-96%-P3HT:PCBM based on oDCB/mesitylene and (e) doctor bladed RR-96%-P3HT:PCBM based on oDCB/mesitylene. A proper resolution could be obtained by adjusting the height amplification to 100 nm for the inkjet printed film (d) and 50 nm for the doctor bladed film (e).

for the equivalent doctor bladed solar cells the doctor blading temperature was set to 60 °C.

Figure 1c represents the AFM image of a doctor bladed RR-93%-P3HT:PCBM film. The inkjet printed layer using the RR-93%-P3HT:PCBM in tetralene (Figure 1b) shows smoother surface compared to RR-98.5%-P3HT:PCBM (Figure 1a), but still too rough and with visible large grain size features in the micrometer scale compared to an optimized RR-93%-P3HT:PCBM doctor bladed layer from tetralene (Figure 1c). The AFM image of the doctor bladed film provides a significantly reduced roughness profile with an rms roughness of 2.4 nm. We attributed the significant distinction in the grain size and surface roughness between RR-93%-P3HT:PCBM inkjet printed and RR-93%-P3HT:PCBM doctor bladed photoactive layers to the different coating temperatures (40 °C for the inkjet table and 60 °C for the doctor blading table) applied during the layer deposition of the formulation from tetralene (see Supporting Information). The AFM image of the inkjet printed RR-93%-P3HT:PCBM layer from tetralene indicates morphological limitations due to a demixing of the polymer and the fullerene within the blend. This can occur if the drying rate is too low by using a low vapor pressure high boiling pristine solvent (tetralene) at a low coating temperature (40 °C). With deficient morphological properties the performance of the photovoltaic device is affected as discussed in more details

later in the text. We note that our trials to fabricate doctor bladed RR-93%-P3HT:PCBM solar cells from tetralene using low deposition table temperature similar to that for our inkjet printed trials exhibit also strong reduction in device performance (see Figure 2 in the Supporting Information).

Due to the above discussion the RR-93%-P3HT:PCBM blend represents the most promising materials for inkjet printing due to longer latency time. Therefore, alternative inkjet printing solvent formulations have been developed for the RR-93%-P3HT:PCBM. The aim of the work was to identify solvent formulations which can achieve higher drying rates and uniform film formation when coated at low temperatures. We found that RR-93%-P3HT:PCBM in 68% of *o*-dichlorobenzene (oDCB) and 32% of 1,3,5-trimethylbenzene (mesitylene) can produce a significantly improved uniformity of an inkjet printed layer with enhanced morphology compared to pristine tetralene and power conversion efficiency of inkjet printed polymer:fullerene blends of 2.9%.[21]

The incorporation of mesitylene into a high boiling point solvent such as oDCB (bp = 180 °C, $vp_{20°C}$ = 1.20 mmHg) is decisive for the inkjet printing technology, because mesitylene possesses a higher vapor pressure for a rapid drying compared to oDCB or tetralene. We show later in the text that this solvent formulation can also produce highly efficient P3HT:PCBM doctor bladed solar cells with low platen temperatures of 40 °C. Thus, the limitation of the low inkjet table coating temperature and slow drying of the inkjet printed blends with high boiling point pristine solvents was overcome by the use of an appropriate solvent mixture. More details on the development of the inkjet mixture concentrations, film properties can be found in detail elsewhere.[21]

It is well-known from the literature that high RR is needed to gain suitable packing of the P3HT polymer chains within the blend after annealing, intimate morphology and high efficiency RR-P3HT:PCBM solar cells.[15] In the case of spin-coated films the higher the RR the better the PCE.[15] As we show above, the high RR-P3HT (98.5%) is not suitable for the inkjet printing technology due to rapid gelling time. Thus, our work was focused on RR-P3HT polymer donors which can combine as high as possible RR with long gelation time for efficient inkjet printed device performance.

Figure 1d,e represents the surface topographies of the RR-96%-P3HT:PCBM with a molecular weight distribution ($M_w$) of 60000 dissolved in oDCB/mesitylene solvent mixture deposited by inkjet printing (Figure 1d) and doctor blading (Figure 1e) processing techniques. In contrast to the strong influence of RR on the gelation time, small variations in molecular weight distribution do not affect the gelation properties.[23] Our printed trials using an ink formulation comprising a high regioregular P3HT (RR-98%) with reduced $M_w$ of 37.000 still result in rapid gelation and low inkjet printing performance.[23] As can be seen in the roughness profile (Figure 1d), a rms roughness of 7.4 nm with a considerably smaller grain size can be achieved for the RR-96%-P3HT:PCBM inkjet printed layer from oDCB/mesitylene formulation, whereas also the control doctor bladed layer based on RR-96%-P3HT:PCBM from oDCB/mesitylene formulation features an ultrasmooth surface with an rms roughness of 3.7 nm, presented in Figure 1e. Hence, by using a RR-96%-P3HT and oDCB/mesitylene solvent mixture the inkjet printed photoactive layer with inkjet table temperature of 40 °C shows similar surface profiles (Figure 1d) to that obtained with the doctor bladed RR-93%-P3HT:PCBM from tetralene (coated at 60 °C) (Figure 1c), but rougher surface topographies compared to doctor bladed RR-96%-P3HT:PCBM from oDCB/mesitylene ink formulation coated at 40 °C (Figure 1e).

As we discussed above due to the longer gelation interval, RR of 93% and 96%-P3HT:PCBM is more suitable for the inkjet printing technology compared to RR-98.5%-P3HT:PCBM. Thus, we focused our device studies on solar cells based on the RR- 93% and 96%-P3HT:PCBM. The device architectures studied are described as follows: Device number 1 is based on inkjet printed RR-93%-P3HT:PCBM using pristine solvents, ITO/doctor bladed PEDOT:PSS/inkjet printed (40 °C) RR-93%-P3HT:PCBM (200 nm) from tetralene/Ca:Ag (device no. 1), device number 2 is the equivalent to device no 1, doctor bladed device, ITO/doctor bladed PEDOT:PSS/doctor bladed (60 °C) RR-93%-P3HT:PCBM (200 nm) from tetralene/Ca:Ag (device no. 2), device number 3 is the inkjet printed RR-96%-P3HT:PCBM device based on a solvent combination of oDCB/mesitylene, ITO/doctor bladed PEDOT:PSS/inkjet printed (40 °C) RR-96%-P3HT:PCBM (230 nm) from oDCB-mesitylene/Ca:Ag (device no. 3) and device number 4 is the doctor bladed equivalent to device no 3., ITO/doctor bladed PEDOT:PSS/doctor bladed (40 °C) RR-96%-P3HT:PCBM (230 nm) from oDCB-mesitylene/Ca:Ag (device no. 4). We note that all devices were subjected to a thermal treatment at 140 °C for 10 min before cathode evaporation, because that was the optimized thermal annealing condition we are using for our highly efficient doctor bladed RR-P3HT:PCBM cells.[20]

Figure 2a,b demonstrates the dark current density/voltage (*J*/*V*) (log-linear plot) and light *J*/*V* under AM 1.5 illumination with 100 mW $cm^{-2}$. Table 1 summarizes the solar cell device performance, rms roughness, active layer thickness and device parameters extracted from the analysis in terms of one-diode equivalent circuit for the four devices under study.[22] The device with a RR-93%-P3HT:PCBM inkjet printed active layer based on pristine tetralene formulation (device no.1, inkjet table temperature 40 °C) demonstrate a short circuit current density ($J_{SC}$) of 4.73 mA/$cm^2$, an open circuit voltage ($V_{oc}$) of 0.45 V, and a fill factor (FF) of 63%. This corresponds to a power conversion efficiency (PCE) of 1.29%. In contrast, the doctor bladed RR-93%-P3HT:PCBM devices based on tetralene solvent formulation (device no. 2, doctor blade table temperature 60 °C) exhibit a higher $J_{SC}$ of 7.87 mA/$cm^2$, a $V_{OC}$ of 0.60 V and a FF of 68%, resulting in a PCE of 3.3%. The devices with a RR-96%-P3HT:PCBM inkjet printed active layer based on oDCB/mesitylene formulation (device no. 3, inkjet table temperature 40 °C) show a short circuit current density ($J_{SC}$) of 10.05 mA/$cm^2$, an open circuit voltage ($V_{oc}$) of 0.537 V, and a fill factor (FF) of 64%. This corresponds to a PCE of 3.47%. This device performance is much higher compared to the

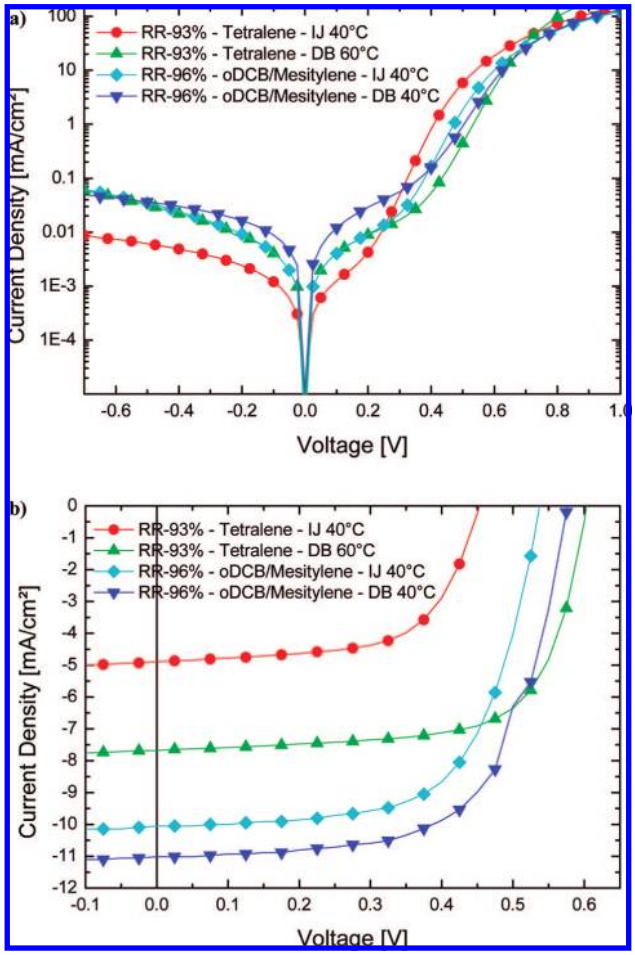


**Figure 2.** current−voltage-characteristics of the different RR-P3HT:PCBM inkjet printed and doctor bladed devices based on either tetralene (red dots and green triangles) or oDCB/mesitylene (dark blue triangles and light blue squares) in the dark (a) and under illumination (b).

RR-93%-P3HT:PCBM inkjet printed device based on tetralene (device no. 1) and oDCB/mesitylene solvent mixture.[21] However, the control doctor bladed RR-96%-P3HT:PCBM devices based on oDCB/mesitylene solvent mixture (device no. 4, doctor blade table temperature 40 °C) has still a higher $J_{SC}$ of 11.15 mA/cm$^2$, a $V_{OC}$ of 0.580 V and a FF of 64%, resulting in a PCE of 4.05%.

From the detailed *J*/*V* simulation[22] we have found that the mobility lifetime ($\mu$-$\tau$) product[22] (Table 1) is in the same range (2.7−4.7) × 10$^{-9}$ cm$^2$/V for all the devices under study. Because the active layer thickness for all tetralene based devices is 200 nm and for all oDCB/mesitylene based devices the film thickness is 230 nm, no clear differences in the FF values (see Table 1) were observed as expected. The differences in the device performance between inkjet printed and doctor bladed cells are mainly due to the lower values for $V_{oc}$ and $J_{SC}$ affecting their PCE.

The higher values of $J_{SC}$ for the doctor bladed solar cells based on tetralene pristine solvent (device 2) compared to inkjet printed cells from tetralene (device 1) is due to the difference in the coating temperature affecting the drying behavior and the film uniformity and, therefore, the morphology of the inkjet printed layer. As we also discussed above

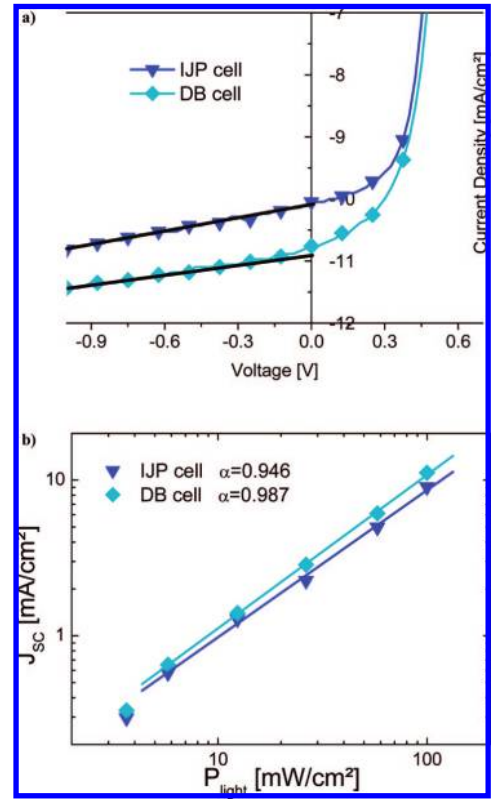


**Figure 3.** Analysis of the losses in the short circuit current of the inkjet printed devices compared to the doctor bladed devices based on the 96% RR-P3HT:PCBM. Figure 3a) voltage dependence measurement of 96% RR-P3HT from oDCB/mesitylene based devices, Figure 3b) illumination intenstiy dependence of 96% RR-P3HT:PCBM devices based on oDCB/mesitylene.

in the text, for the RR-93%-P3HT:PCBM we have found that inkjet table temperatures of 40 °C result in the most uniform film within one printed area and more reliable printing regarding the wetting behavior and film formation for both formulations studied. Higher inkjet table temperatures result in a suppressed film formation and, therefore, a dewetting of the inkjet printed layer due to an unfavorable surface behavior of the substrate. The limitation in the performance of inkjet printed cells based on pristine solvent can be attributed to the low deposition temperatures (40 °C) of the inkjet table for the comparatively high-boiling solvent, such as tetralene used in this study negatively affecting the P3HT:PC$_{61}$BM morphology and surface roughness due to demixing of the materials within the blend during the drying process.[23]

To assess the losses in the short circuit current density between the highest efficient inkjet printed (device 3) and doctor bladed (device 4) devices, the solar cells based on RR-96% and oDCB/mesitylene mixture were subjected to an illumination intensity and voltage dependence measurement.[24] The experimental data for the analysis in terms of voltage dependence for the inkjet printed and doctor bladed solar cells are presented in Figure 3a, and the light intensity measurements of the inkjet printed and doctor bladed solar cells are presented in Figure 3b. Considering figure 3b, the double logarithmic representation shows the dependence of the $J_{sc}$ on the illumination intensity. The linear fit of the

**Table 1.** RR, Device Performance, rms Roughness, Active Layer Thickness, Deposition Temperature and Mobility Lifetime Product Extracted from the Analysis of Devices Using One-Diode Equivalent Circuit[22] of the Inkjet Printed and Doctor Bladed Devices Based on Either 93% RR-P3HT from Tetralene (Device 1 and 2) or 96% RR-P3HT from oDCB/Mesitylene (Devices 3 and 4)

| | RR-93%-tetralene IJ device 1 | RR-93%-tetralene DB device 2 | RR-96%-oDCB/mesitylene IJ device 3 | RR-96%-oDCB/mesitylene DB device 4 |
|---|---|---|---|---|
| regioregularity of P3HT [%] | 93 | 93 | 96 | 96 |
| PCE [%] | 1.29 | 3.3 | 3.47 | 4.05 |
| FF | 0.63 | 0.68 | 0.64 | 0.64 |
| $J_{sc}$ [mA/cm$^2$] | 4.73 | 7.87 | 10.05 | 11.15 |
| $V_{oc}$ [mV] | 450 | 600 | 537 | 580 |
| rms roughness [nm] | 26.0 | 2.4 | 7.4 | 3.7 |
| active layer thickness [nm] | 200 | 200 | 230 | 230 |
| deposition temp [°C] | 40 | 60 | 40 | 40 |
| $\mu\tau$-product [cm$^2$/V] | $4.7 \times 10^{-9}$ | $3.0 \times 10^{-9}$ | $2.7 \times 10^{-9}$ | $3.1 \times 10^{-9}$ |

measurement data reveals slopes of 0.95 for device no. 3 and 0.99 for device no. 4. The smaller slope of the inkjet printed devices (device no 3) compared to the doctor bladed device (device 4) is an indication of the presence of second-order recombination for the inkjet printed device.

Due to experimental uncertainty, the voltage dependent measurement (Figure 3a) cannot provide any clear differences due to recombination of first order for both devices, independent of the coating technique. Therefore, the lower values of $J_{SC}$ and $V_{oc}$ for the doctor bladed cells based on the 96% RR and the solvent mixture can be related to the presence of bimolecular recombination losses. Despite this, the inkjet printed devices are not fully optimized. Further improvements can be achieved by optimizing the P3HT:PCBM concentration, annealing temperatures and, importantly, more detailed donor tuning of the chemical properties to achieve the highest possible regioregularity for intimate morphology with adequate gelation time for printing.

In summary, we have shown that morphology induced contrast of inkjet printed solar cells to the major findings of high PCE P3HT:PCBM solar cells fabricated by spin coating or doctor-blading techniques, where highest RR,[15] slow drying[14] and pristine chlorinated solvents[20] are essential conditions to achieve a high PCE performance. For inkjet printing we have found that the chemical properties of RR-P3HT have to be readjusted to extend the gelation time and provide suitable morphology during the inkjet printed process.

To conclude, we demonstrate that the inkjet printing technology requires film formation and drying conditions which are fundamentally different compared to conventional coating techniques such as doctor blading or spin coating. By using the combination of a RR-96%-P3HT and an adapted solvent mixture oDCB/mesitylene to control the drying and film formation, we have achieved suitable gelation time, improved the morphological properties of the active layer and achieved 3.5% PCE inkjet printed polymer:fullerene based solar cells. Development of suitable formulation of functional multi component inks, to control the morphology of bulk-heterojunction solar cells during the printing process is an essential step for the commercialization of organic photovoltaics.

**Inkjet Printing and Experimental Methods.** Direct comparison between the doctor blading and spin coated process as well as experimental details for the process techniques of doctor blading have been published in detail elsewhere.[20] In this study the patterning of the RR-P3HT:PCBM photoactive layer was performed by the inkjet printing technique using a commercial piezoelectric driven inkjet head with a motorized xyz stage, a fiducial camera for the substrate alignment and a drop watcher camera to control the drop shape (from Fujifilm Dimatix, Inc.). These inkjet printed photovoltaic devices were compared with doctor bladed devices. To have a reliable printing, the inks should demonstrate a stable jetting behavior. To be compatible with the print head, the fluids must fulfill certain requirements such as viscosity in the range 1−30 mPas to ensure that formulation can be jetted reliably from the print head and low surface tensions, 30−40 dyn/cm$^2$, resulting in good wetting of the ink on the PEDOT:PSS underlayer. Best outcome was obtained with very low viscosities up to 10 mPas. Therefore, semiconducting inks, concluding a blend of RR-P3HT and PCBM, were formulated that meet the above specifications.

A critical parameter for the inkjet printing process is the gelation time of the polymer:fullerene organic solvent based ink. Because the nozzles of the print head are open to the atmosphere, when not printing, the solvent will evaporate causing an increase in the ink viscosity around the nozzles. Due to the viscosity increase, gelation of the blend solution will occur. This chemical modification of the ink reduces the latency time of the blend solution and results in a higher solute concentration at the nozzle orifice and thus, the droplet parameters are shifted affecting the reliability of the printing in terms of droplet volume, velocity and angularity. The time interval until the ink is chemically modified (e.g., gelation of the blend solution) is called the latency time of an ink, and the time interval at which printing can continuously proceed up to nozzle clogging is called the dwell time of an ink. Although the side chains of the polythiophene are responsible for the solubility, the rigid nature of the RR-P3HT polymers backbone can cause gelation problems in the blend with fullerenes if the chemical properties of the RR-P3HT are not carefully controlled. We showed in the text that the latency time of an inkjet RR-P3HT:PCBM formulation

can be controlled by the chemical properties of the RR-P3HT donor such as the regioregularity.

The droplet formation is very dependent on both the rheology of the blend solution and the driving conditions of the print head. The jetting frequency and the driving voltage has to be matched with the fluid and were thus adjusted to achieve a stable jetting, the best droplet formation with a drop velocity ranging from 6 to 9 m/s and a droplet volume in the order of 10 pL. A fine-tuning of the driving conditions allows a decrease in satellites and tailing of the droplets. The jetting of the print head operates under negative pressure to keep the meniscus at the edge of the nozzle, depending on the viscosity and surface tension of the ink. The film thickness of the dried layer was finally adjusted by varying the drop spacing. Figure 3 in the Supporting Information presents the correlation between drop distance and the inkjet printed layer thickness. The arrow in Figure 3 (Supporting Information) emphasizes the parameters graphically used for the device fabrication. For the inkjet printed RR-93%-P3HT:PCBM tetralene based solution the drop spacing was adjusted to 30 $\mu$m, whereas for the RR-96%-P3HT:PCBM oDCB/mesitylene based ink the distance between each droplet was set to 35 $\mu$m. With these conditions the printed layers demonstrate the most uniform film with fewest thickness variations within one printed area and a reliable printing regarding the spreading and film formation could be achieved.

The devices were built on transparent indium tin oxide (ITO) coated glass substrates. The glasses were cleaned 10 min in acetone and another 10 min in isopropyl alcohol using an ultrasonic bath and finally with a 10 min lasting ozone treatment. A thin 60 nm layer of poly(3,4-ethylenedioxythiophene) doped with polystyrene sulfonic acid (PEDOT:PSS) was deposited by doctor blading on top of the ITO bottom electrode and the freshly coated layers were stored in a vacuum chamber for a couple of hours. For our devices the Baytron PH purchased from H. C. Starck was used, comprising a PEDOT:PSS ratio of 1:2.5 by weight. After the PEDOT:PSS doctor blading step, the samples were placed 1 mm below the inkjet print head for the coating of the photoactive layer by the Fujifilm Dimatix commercial inkjet printing tool. The semiconducting solution consists of 1 wt % P3HT (poly(3-hexylthiophene)) blended with the fullerene $PC_{61}BM$ ([6,6]-phenyl $C_{61}$ butyric acid methyl ester) in a ratio of 1:1 by weight were dissolved in either tetralene or oDCB/mesitylene solvent mixture. On top of the active layer, an additional Ca:Ag top electrode was deposited by physical vapor deposition to complete the bulk heterojunction solar cell. For solar cell efficiency evaluation the device area was defined by the overlap between the underlying ITO and the top electrode. Solar cells with an active area of typically 20 $mm^2$ and up to 1 $cm^2$ were studied. Devices current density−voltage ($J-V$) characteristics were assessed with a source measurement unit SMU 2400 from Keithley under nitrogen atmosphere. For illumination a Steuernagel solar simulator was used providing an AM 1.5G spectra at 0.1W/$cm^2$. The Steuernagel solar simulator is equipped with metal halogenide lamps. The mismatch factor of the solar simulator to P3HT:PCBM based solar cells was assessed by cross calibrating to external quantum efficiency measurements. A mismatch factor of 0.75 was determined. All efficiency performance values in this paper have been calculated using a mismatch of 0.75.

The high-resolution atomic force microscope consists of a cantilever with a sharp tip at its end to scan the surface of the sample. The probe was based on silicon nitride with a radius of curvature in the nanometer scale.

**Acknowledgment.** We thank Christoph Waldauf and Prof. Juergen Parisi for valuable discussions. The work was performed at Konarka Technologies Gmbh. All the experimental work including selection of solvent formulations was performed by C.N.H. as part of her Ph.D. Thesis. C.N.H. also contributed to *J*/*V* simulations and experimental design. P.S. performed the *J*/*V* simulations and contributed to the experimental design. S.A.C. was the supervisor of C.N.H. at Konarka Technologies and contributed to experimental design and project planning. He completed the device physics part of the manuscript after he joined the Department of Mechanical Engineering and Materials Science and Engineering at the Cyprus University of Technology. C.J.B. initiated the inkjet printing project at Konarka Technologies and contributed to experimental design and project planning.

**Supporting Information Available:** Graphs of current−voltage characteristics of 98.5% RR-P3HT:PCBM–tetralene device, comparison of doctor bladed 93% RR-P3HT:PCBM tetralene formulation deposited at different coating temperatures and correlation of inkjet printing drop spacing and active layers film thickness. This material is available free of charge via the Internet at http://pubs.acs.org.

## References

(1) Sariciftci, N. S.; Smilowitz, L.; Heeger, A. J.; Wudl, F. Photoinduced Electron Transfer from a Conducting Polymer to Buckminsterfullerene. *Science* **1992**, *258*, 1474–1476.
(2) Halls, J. J. M. Efficient photodiodes from interpenetrating polymer networks. *Nature* **1995**, *376*, 498–500.
(3) Yu, G.; Gao, J.; Hummelen, J. C.; Wudl, F.; Heeger, A. J. Polymer Photovoltaic Cells: Enhanced Efficiencies via a Network of Internal Donor-Acceptor Heterojunctions. *Science* **1995**, *270*, 1789–1791.
(4) Brabec, C. J.; Hauch, J. A.; Schilinsky, P.; Waldauf, C. Production Aspects of Organic Photovoltaics and Their Impact on the Commercialization of Devices. *MRS Bull.* **2005**, *30*, 50.
(5) Hoppe, H.; Sariciftci, N. S. Organic solar cells: An overview. *J. Mater. Res.* **2004**, *19*, 1924–1945.
(6) Kim, Y.; et al. Device annealing effect in organic solar cells with blends of regioregular poly(3-hexylthiophene) and soluble fullerene. *Appl. Phys. Lett.* **2005**, *86*, 063502.
(7) Beek, W. J. E.; Wienk, M. M.; Janssen, R. A. J. Hybrid Solar Cells from Regioregular Polythiophene and ZnO Nanoparticles. *Adv. Funct. Mater.* **2006**, *16*, 1112–1116.
(8) Shaheen, S. E. 2.5% efficient organic plastic solar cells. *Appl. Phys. Lett.* **2001**, *78*, 841–843.
(9) Padinger, F.; Rittberger, R. S.; Sariciftci, N. S. Effects of postproduction treatment on plastic solar cells. *Adv. Funct. Mater* **2003**, *13*, 85–88.
(10) Waldauf, C.; et al. Highly efficient inverted organic photovoltaics using solution based titanium oxide as electron selective contact. *Appl. Phys. Lett.* **2006**, *89*, 233517.
(11) Kim, Y. Composition and annealing effects in polythiophene/fullerene solar cells. *J. Mater. Sci.* **2005**, *40*, 1371–1376.
(12) Ma, W. L.; Yang, C. Y.; Gong, X.; Lee, K.; Heeger, A. J. Thermally stable, efficient polymer solar cells with nanoscale control of the interpenetrating network morphology. *Adv. Funct. Mater* **2005**, *15*, 1617–1622.

(13) Reyes-Reyes, M. Meso-Structure Formation for Enhanced Organic Photovoltaic Cells. *Org. Lett.* **2005**, *7*, 5749–5752.
(14) Li, G.; et al. High-efficiency solution processable polymer photovaoltaic cells by self-organization of polymer blends. *Nat. Mater.* **2005**, *4*, 864–868.
(15) Kim, Y. A strong regioregularity effect in self-organizing conjugated polymer films and high-efficiency polythiophene:fullerene solar cells. *Nature Mater.* **2006**, *5*, 197–203.
(16) Schilinsky, P.; Asawapirom, U.; Scherf, U.; Biele, M.; Brabec, C. J. Influence of the Molecular Weight of Poly(3-hexylthiophene) on the Performance of Bulk Heterojunction Solar Cells. *Chem. Mater.* **2005**, *17*, 2175–2180.
(17) Kim, Y. Effect of the end group of regioregular poly(3-hexylthiophene) polymers on the performance of polymer/fullerene solar cells. *J. Phys. Chem. C* **2007**, *111*, 8137–8141.
(18) Kim, Y.; et al. Polymer chain/nanocrystal ordering in thin films of regioregular poly(3-hexylthiophene) and blends with a soluble fullerene. *Soft Matter* **2006**, *3*, 117–121.
(19) Peet, J. Efficiency enhancement in low-bandgap polymer solar cells by processing with alkane dithiols. *Nat. Mater.* **2007**, *6*, 497–500.
(20) Schilinsky, P.; Waldauf, C.; Brabec, C. J. Performance analysis of printed bulk heterojunction solar cells. *Adv. Funct. Mater* **2006**, *16*, 1669–1672.
(21) Hoth, C. N.; Choulis, S. A.; Schilinsky, P.; Brabec, C. J. High Photovoltaic Performance of inkjet printed polymer:fullerene blends. *Adv. Mater.* **2007**, *19*, 3973–3978.
(22) Waldauf, C.; Scharber, M. C.; Schilinsky, P.; Hauch, J. A.; Brabec, C. J. Physics of organic bulk heterojunction devices for photovoltaic applications. *J. Appl. Phys.* **2006**, *99*, 104503.
(23) Hoth, C. N., Schilinsky, P., Choulis, S. A. & Brabec, C. J. in preparation(2008).
(24) Schilinsky, P. Ph.D. Thesis, University of Oldenburg, Germany, 2005.
(25) Shaheen, S. E.; Radspinner, R.; Peyghambarian, N.; Jabbour, G. E. *Appl. Phys. Lett.* **2001**, *79* (18), 2996.
(26) Tuomikoski, M.; Kopola, P. *Technologies for Polymer Electronics TPE 06*; Rudolstadt, Germany, 16−18 May 2006.
(27) Nie, Z.; Kumacheva, E. *Nat. Mater.* **2008**, 7.

NL801365K